HEFAT2010
7th International Conference on Heat Transfer, Fluid Mechanics and Thermodynamics
19-21 July 2010
Antalya, Turkey

COMBINED NATURAL CONVECTION ENHANCEMENT IN RIGHT-ANGLED TRIANGULAR CAVITIES USING HELIUM AND SURFACE RADIATION

Antonio Campo[a*+] and Jaime Sieres[b]
[b]The University of Texas at San Antonio, Department of Mechanical Engineering, San Antonio, TX 78249, USA
[a]Universidad de Vigo, Área de Máquinas y Motores Térmicos, ETSII, Campus Lagoas-Marcosende nº 9, 36310 Vigo, Spain

*E-mail: antonio.campo@utsa.edu

ABSTRACT

The present investigation deals with the numerical computation of laminar natural convection in upright-angled triangular cavities filled with helium. In each cavity, the vertical wall is heated and the inclined wall is cooled while the upper horizontal wall is thermally insulated from the ambient air. The defining aperture angle φ is located at the lower vertex between the vertical and inclined walls. To incorporate surface radiation, various levels of emissivities are assigned to the walls. The finite volume method is implemented to perform the computational analysis encompassing three aperture angles φ (= 15º, 30º and 45º) in conjunction with height-based Rayleigh numbers ranging from a low 10^3 to a high 10^6. Numerical results for helium with and without surface radiation are reported for the buoyant velocity and temperature fields as well as the mean convective coefficient at the heated vertical wall.

NOMENCLATURE

B	[W/m^2]	Radiosity
c_p	[kJ/kgK]	Specific isobaric heat capacity
F_{ij}	[-]	View factor from segment i to segment j
g	[m/s^2]	Gravitational acceleration
G	[W/m^2]	Irradiation
h	[W/m^2]	Convective coefficient
k	[W/mK]	Thermal conductivity
L	[m]	Length of wall
n	[-]	Total number of boundary differential segments
Nu	[-]	Nusselt number, $Nu = h \cdot L_H/k$
p	[Pa]	Pressure
q	[W/m^2]	Heat flux
R_{air}	[J/kgK]	Gas constant
Ra	[-]	Rayleigh number, $Ra = g \cdot \beta \cdot (T_H - T_C) \cdot L_H^3/(\alpha \cdot \upsilon)$
s	[m]	Distance along the wall
T	[K]	Absolute temperature
u, v	[m/s]	Velocity components in the x and y directions
x, y	[m]	Horizontal and vertical Cartesian coordinates

Special characters

α	[m^2/s]	Thermal diffusivity
β	[1/K]	Coefficient of volumetric thermal expansion
δ_{ij}	[-]	Kronecker delta
ΔT	[K]	Prescribed temperature difference, $(T_H - T_C)$
ε	[-]	Total hemispherical emissivity
θ	[-]	Dimensionless temperature, $(T_H - T_C)/\Delta T$
μ	[kg/ms]	Dynamic viscosity
υ	[m^2/s]	Kinematic viscosity
ρ	[kg/m^3]	Density
σ	[W/m^{2}K^4]	Stefan-Boltzmann constant
φ	[rad]	Aperture angle
ψ	[kg/s]	Stream function

Subscripts

0	Reference value
A	Adiabatic
C	Cold
cri	Critical
H	Hot
i, j	Element indexes

Superscripts

$-$	Mean value at the wall

INTRODUCTION

The upright right-angled triangular cavities find application in the miniaturization of cabinets housing electronic components that are severely constrained by space and/or weight. With a view at enhancing the heat transfer rates and/or reducing the size of cabinets, the influence that surface radiation exerts upon natural convection has to be scrutinized. Representative references of this effort for natural convection in square cavities are those of Balaji and Venkateshan [1], Akiyama and Chong [2], Ramesh and Venkateshan [3] and Wang, Xin and Le Quéré [4].

Sieres at al. [5] undertook for the first time the numerical computation of laminar natural convection with surface radiation in upright-angled triangular cavities filled with air. The vertical walls were heated and the inclined walls were cooled with adiabatic upper connecting walls. The aperture angle φ located at the lower vertex of the triangular cavities between the vertical and the inclined walls identifies the shape of each cavity. In this work, the finite volume method was employed to perform the computational analysis. Numerical

results were reported for the local quantities, the velocity and temperature fields encompassing aperture angles φ that extend from 15° to 45° at two extreme Rayleigh numbers, $Ra = 10^3$ and 10^6. Additionally, the two global quantities, the mean convective Nusselt number and the mean radiative Nusselt number were reported in tabulated and graphical forms for the controlling parameters. Overall, it was found that the competition between surface radiation and natural convection in this kind of triangular cavities filled with air plays a preponderant role in the heat transfer performance. The analysis culminated with a comprehensive correlation equation for the total Nusselt number in terms of the controlling parameters which should be useful for engineering analysis and design.

When the design criteria for natural convection cavities calls for heat transfer enhancement and weight limitations, a literature review (Raithby and Hollands [6], Jaluria [7]) reveals that there is no information available with regards to gases that perform better than air. Therefore, the intent of the present work is to fill this gap and investigate the attributes of helium as the working fluid coupled when surface radiation in upright-angled triangular cavities.

Other attempts to enhance heat transfer in cavities have been explored using porous media. Steady-state free convection heat transfer in a right-angle triangular enclosure, whose vertical wall insulated and inclined and bottom walls are differentially heated was performed by Varol et al. [8]. The governing equations relying on the Darcy model were solved by finite difference method and solution of algebraic equations was made via the Successive under Relaxation method. The effect of aspect ratios ranging from 0.25 to 1.0 and Rayleigh numbers within $50 \le Ra \le 1000$ was investigated as the controlling parameters of the flow and temperature fields. It was observed that heat transfer was increased with reductions in the aspect ratio. Additionally, multiple cells were formed at high Rayleigh numbers.

PHYSICAL SYSTEM AND MATHEMATICAL MODEL

The physical system to be considered in this study is depicted in Figure 1. It consists of a right-angled triangular cavity oriented vertically filled with helium. The three walls are impermeable, the vertical wall of length L_H is heated, the inclined wall of length L_C is cooled while the upper connecting horizontal wall of length L_A is thermally insulated. The defining aperture angle φ is located at the lower vertex between the heated vertical and the cooled inclined walls. Values of the total hemispherical emissivity at the three surfaces are contained between the limiting cases 0 and 1.

In the triangular cavity, the longitudinal dimension perpendicular to the paper is assumed very long when compared with the dimensions defining the cross section. Owing to this proportionality, the natural convection problem is conceived to be two-dimensional.

The gravitational acceleration g acts in the vertical direction. The mathematical model for steady-state buoyant flow with Boussinesq approximation is expressed by the following system of conservation equations:

Figure 1 (a) Sketch of the right-angled triangular cavity, (b) energy balance in a differential segment of the top horizontal wall.

Mass conservation:

$$\frac{\partial(\rho \cdot u)}{\partial x} + \frac{\partial(\rho \cdot v)}{\partial y} = 0 \tag{1}$$

Momentum equation in x:

$$\frac{\partial(\rho \cdot u \cdot u)}{\partial x} + \frac{\partial(\rho \cdot v \cdot u)}{\partial y} = -\frac{\partial P}{\partial x} + \frac{\partial(\mu \cdot \partial u/\partial x)}{\partial x} + \frac{\partial(\mu \cdot \partial u/\partial y)}{\partial y} \tag{2}$$

Momentum equation in y:

$$\frac{\partial(\rho \cdot u \cdot v)}{\partial x} + \frac{\partial(\rho \cdot v \cdot v)}{\partial y} = -\frac{\partial P}{\partial y} + \frac{\partial(\mu \cdot \partial v/\partial x)}{\partial x} + \frac{\partial(\mu \cdot \partial v/\partial y)}{\partial y} + g \cdot (\rho - \rho_0) \tag{3}$$

Energy conservation:

$$\frac{\partial(\rho \cdot c_p \cdot u \cdot T)}{\partial x} + \frac{\partial(\rho \cdot c_p \cdot v \cdot T)}{\partial y} = \frac{\partial(k \cdot \partial T/\partial x)}{\partial x} + \frac{\partial(k \cdot \partial T/\partial y)}{\partial y} \tag{4}$$

Ideal gas equation of state:

$$\rho = p \cdot R_{air} \cdot T \tag{5}$$

In the buoyancy term of Eq. (3), ρ_0 stands for a reference density evaluated at a reference temperature $T_0 = (T_H + T_C)/2$.

The velocity boundary conditions are linked to the no slip condition at the impermeable walls, implying $u = v = 0$. The thermal boundary conditions are established by two prescribed temperatures: T_H at the hot vertical wall and T_C at the cold inclined wall. At the top horizontal wall, the heat flux must be zero to comply with a thermally insulated condition.

Within the platform of surface radiation, there are two distinct cases at the top wall. First, if surface radiation is inactive, the thermal boundary condition is simply expressed as

$$\frac{\partial T}{\partial y} = 0 \tag{6}$$

Second, when surface radiation is active, a suitable thermal boundary condition must be constructed. Thereby, the energy balance over a differential wall segment i in Figure 1(b) is stated as

$$q_{V,i} + q_{R,i} = q_{V,i} + G_i - B_i = 0 \tag{7}$$

where $q_{V,i}$ is the local convective heat flux that results from applying Fourier's law to the temperature field, $q_{R,i}$ is the local radiative heat flux, G_i is the irradiation falling on the differential segment i and B_i is the radiosity leaving the segment. As far as the radiosity B_i is concerned, this quantity can be expressed as the sum of the radiation emitted by the wall segment and the irradiated energy reflected by it. For instance, for an opaque grey surface, B_i can be expressed as:

$$B_i = \varepsilon_i \cdot \sigma \cdot T_i^4 + (1 - \varepsilon_i) \cdot G_i \tag{8}$$

where ε_i is the total hemispherical emissivity, σ is the Stefan-Boltzmann constant and T_i is the temperature of the differential wall segment.

The irradiating heat $A_i G_i$ falling on the segment i can be obtained as the sum of the fraction of the heat emitted from all the other surfaces forming the triangular cavity that reaches the segment i. That is,

$$A_i \cdot G_i = \sum_{j=1}^{n} A_j \cdot G_j \cdot F_{ji} \tag{9}$$

Alternatively, by virtue of the reciprocating rule, the following relation

$$\sum_{j=1}^{n} \left[\delta_{ij} - (1 - \varepsilon_i) \cdot F_{ji}\right] \cdot B_j = \varepsilon_i \cdot \sigma \cdot T_i^4 \tag{10}$$

is obtained where δ_{ij} is the Kronecker delta, n is the total number of segments and F_{ij} is the view factor from segment i in the adiabatic wall to the segment j in the other walls. The summation term in Eq. (10) is to be taken for all the elements j with which the element i can interact radiatively.

NUMERICAL COMPUTATION AND VALIDATION

The system of partial differential equations (1)-(4), subject to the imposed velocity and thermal boundary conditions is discretized with the finite volume method (Patankar [9] and Versteeg and Malalasekera [10]) in a computational domain that is coincident with the physical domain. As usual, the discretization of the convective term in the conservation equations is accomplished by the second-order-accurate QUICK scheme, while the pressure-velocity coupling is handled with the SIMPLE scheme [9].

The energy balance over every segment i along the adiabatic wall is expressed by Eq. (7) and requires the solution of the system of algebraic equations as given by Eq. (10). However, to carry out this solution, previous knowledge of the segment temperature T_i, the wall total hemispherical emissivities ε_i and the view factors F_{ij} are needed beforehand. The emissivity values are input parameters depending on the surface characteristics. Calculations of the view factors were performed before the beginning of the iteration procedure, because they depend on the geometry only. The wall temperatures are updated at each iteration of the discretized energy equation.

With regards to the mesh, a sequence of numerical experiments was performed with different grid sizes that ranged from a minimum 10,000 up to a maximum 80,000 triangular elements. A mesh of 40,000 elements was chosen as adequate because it rendered grid independent velocity and temperature fields for the critical cases tested. Care was taken to gradually increase the element density in vulnerable areas where high velocity gradients and/or high temperature gradients would occur, such as near the bounding walls and in the cavity corners. In order to avoid a temperature discontinuity at the intersection between the hot and cold walls, the lower corner was replaced with a very small adiabatic strip that does not affect the velocities and temperatures in this sub-region. At the end, global convergence was guaranteed by controlling the residuals of the conservation equations setting its variations to less than 10^{-6}.

RESULTS AND DISCUSSION

The collection of numerical values of $u(x, y)$, $v(x, y)$ and $T(x, y)$ depends on four factors: (1) the shape and dimension of the triangular cavity, (2) the working fluid (air and helium), (3) the imposed temperature difference $T_H - T_C$ and (4) the wall surface emissivities ($0 < \varepsilon_i < 1$). The shape and dimension can be defined with the height of the triangular cavity L_H and the sweeping aperture angle φ. If the cavity height and the temperature difference are merged with the buoyant-to-viscous forces ratio, this combination leads to the height-based Rayleigh number Ra. Thus, at a first glance, the heat transfer performance of the cavity could be expressed as a function of the Rayleigh number and the aperture angle φ only. However, when radiation interaction is considered, these parameters in conjunction with one of the temperatures T_H or T_C has to be specified as well as the surface emissivities. Moreover, Sieres et al. [5] have shown that when using air as the working fluid, surface radiation alters the velocity and temperature fields, leading to an elevation in the convective Nusselt number on the hot vertical wall. In view of this, we have retained the contribution of the thermophysical properties of the working fluid. Besides, we have considered the heat transfer performance of the cavity being dependent on the Rayleigh number Ra, the aperture angle φ, the wall emissivities and one of the two participating temperatures T_H or T_C.

In this paper, numerical results are reported for three different aperture angles $\varphi = 15^\circ$, 30° and 45°. For the three distinct cavities, the height-based Rayleigh number was varied from a low $Ra = 10^3$ to a high $Ra = 10^6$. The computations were performed at standard atmospheric pressure, using helium as the working fluid. In order to analyze the effect of helium, the

results are compared with those obtained for air by Sieres et al. [5]. Owing that perfect gas behaviour was assumed, the thermal expansion coefficient β is given by $1/T_0$. The properties of helium over the operating temperature interval were obtained from REFPROP [11]. The peculiar characteristics of helium can be summarized as follows: the thermal conductivity of helium is 5.5 times that of air, the density of helium is 0.1 times that of air, the specific heat of helium is 5 times that of air whereas the dynamic viscosity are comparable.

The hot and cold wall temperatures were set to fixed values of 313 K and 287 K, respectively. To asses the contribution of surface radiation, the surface emissivities were allowed to vary from 0 (highly polished surface) to 1 (pure black surface). It should be noted that the effect of the temperature difference must also be analyzed when radiation interaction is considered. However, because of page limitation, this effect is not analyzed in this paper and will be considered in a future work.

In Figure 2, the velocity and temperature contours at a low $Ra = 10^3$ for the three aperture angles $\varphi = 15^\circ$, 30° and 45° are shown when pure natural convection is considered (blue lines) and when surface-to-surface radiation with $\varepsilon = 1$ is incorporated in the analysis (red lines). Table 1 contains the numerical results of the maximum stream function values for the cases analyzed.

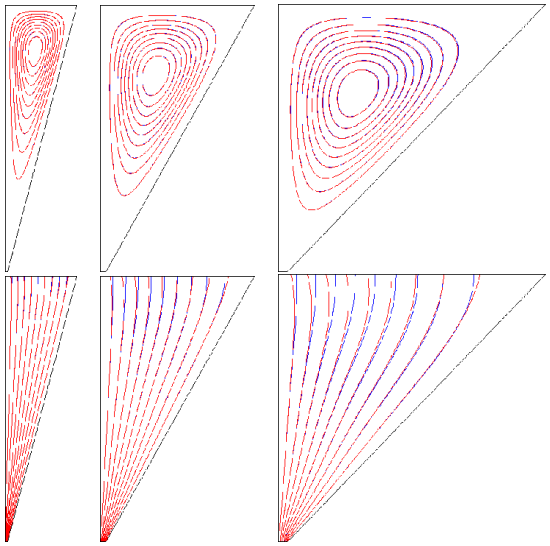

Figure 2 Streamlines and isotherms (θ) related to natural convection (blue lines) and combined natural convection with radiation (red lines) for a low $Ra = 10^3$ and three aperture angles 15º, 30º and 45º ($\Delta\psi = \psi_{max}/10$, $\Delta\theta = 0.1$)

The pair of velocity fields $u(x, y)$, $v(x, y)$ for the tree cavities shows that these configurations contain a single clockwise rotating vortex, which takes the shape of the cavity. The vortex moves the warm fluid from the left vertical wall along the top of the cavity and then down along the cold inclined wall. It is evident from the figure that when the aperture angle is increased, the vortex moves down toward the bottom corner of the cavity. Also from the numbers in Table 1, it is concluded that the stream function gradient is higher in the 45º cavity than in the 30º and 15º cavities; i.e., the streamlines are denser, which means that the velocity values are also higher. In addition, both Table 1 and Figure 2 demonstrate that the effect of surface radiation in the velocity fields $u(x, y)$, $v(x, y)$ is negligible.

Switching to the temperature field $T(x, y)$, it can be seen that the main orientation of the isotherms is vertical which denotes that the process is highly dominated by conduction. The temperature contours for pure natural convection and convection-radiation interaction are almost identical, with the exception that the isotherms are inclined towards the hot or cold wall in the upper region of the triangular cavity. This behaviour is due to the nature of the boundary condition at the top adiabatic horizontal wall, which implies an outward radiative heat transfer near the hot wall and an inward radiative heat transfer near the cold wall. Finally, it can be observed that the isotherms are perpendicular to the top horizontal wall, in concordance with the imposed adiabatic boundary condition.

Table 1

Maximum stream function values for the cases analyzed

φ	Ra	ε	ψ_{max}
15º	10^3	0	$7.47 \cdot 10^{-7}$
		1	$7.47 \cdot 10^{-7}$
	10^6	0	$3.33 \cdot 10^{-4}$
		1	$3.42 \cdot 10^{-4}$
30º	10^3	0	$3.92 \cdot 10^{-6}$
		1	$3.91 \cdot 10^{-6}$
	10^6	0	$4.99 \cdot 10^{-4}$
		1	$5.39 \cdot 10^{-4}$
45º	10^3	0	$9.46 \cdot 10^{-6}$
		1	$9.46 \cdot 10^{-6}$
	10^6	0	$5.26 \cdot 10^{-4}$
		1	$5.72 \cdot 10^{-4}$

Figure 3 illustrates the same results displayed in Figure 2, but for a high $Ra = 10^6$. When comparing the streamlines of the three cavity configurations in this figure with those in Figure 2, it is clear that the vortices have moved down toward the bottom corner of the cavity. The results listed in Table 1 indicate that the stream function gradients are again higher in the 45º cavity than those in the 30º and 15º cavities. Moreover, now the stream function values are increased by two orders of magnitude when compared with the $Ra = 10^3$ case. This increment in the velocity field translates into the fluid flow being dominated by natural convection. As a consequence, now the temperature field is strongly influenced by the velocity field and the isotherms in Figure 3 are arranged horizontally instead of vertically in the core of the cavity.

With respect to the effect of surface radiation, it is clear from Figure 3 that radiation modifies the velocity and temperature fields. Moving from the bottom of the cavity to the top, the isotherms are analogous to the ones found without convection-radiation interaction. However, when approaching

the top adiabatic wall, the effect of radiation heat is noticeable as it tends to cool the hot air layers, leading to a more homogenous temperature field inside the cavity. In fact, there is unstable stratification close to the top wall (i.e., cold air over hot air) and even though in the core of the cavity stable stratification occurs, it is weaker than that for pure natural convection (i.e., larger separation between isotherms). This pattern is pronounced for the 45º and 30º cavities, where higher velocity values are obtained. However, it is less important for the 15º cavity where the streamlines are almost identical and the isotherms are mainly unaffected in the core of the cavity.

Conversely, radiation also affects the velocity field inside the cavity, especially near the top where it can be perceived that the streamlines are flattened when compared with their counterparts for pure convection. Moreover, the numbers in Table 1 reflect that the stream function gradient is slightly higher with radiation interaction, so higher velocities and vigorous heat transfer coefficients are expected.

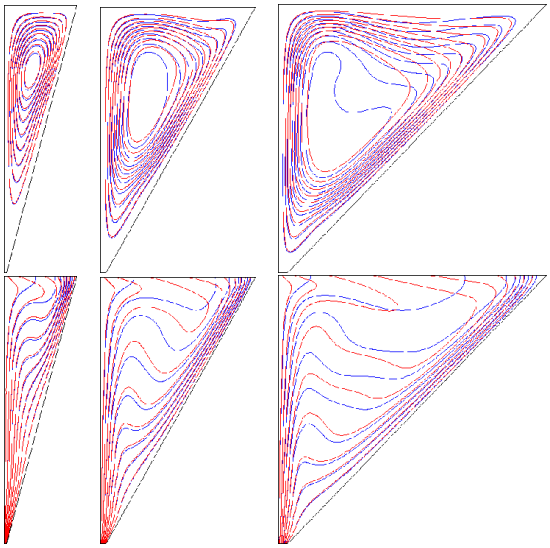

Figure 3 Streamlines and isotherms (θ) related to natural convection (blue lines) and combined natural convection with radiation (red lines) for a high $Ra = 10^6$ and three aperture angles 15º, 30º and 45º ($\Delta\psi = \psi_{max}/10$, $\Delta\theta = 0.1$)

For the purpose of analyzing the heat transfer features of the three cavities, the Nusselt number on the hot vertical wall is calculated by

$$Nu = \frac{q(s)\cdot L_H}{k\cdot\Delta T} \tag{11}$$

where s represents the distance measured along the hot wall where L_H is its length, $q(s)$ is the local wall heat flux along the hot wall and the thermal conductivity k is evaluated at the reference temperature T_0. Subsequently, the mean Nusselt number can be obtained as

$$\overline{Nu} = \frac{1}{L_H}\cdot\int_0^{L_H} Nu(s)\cdot ds \tag{12}$$

Due to a superabundance of parameters, the mean Nusselt numbers on the hot wall are plotted in Figure 4 as a function of the Rayleigh number for the three aperture angles 15º, 30º and 45º and for the two limiting conditions of pure natural convection ($\varepsilon = 0$) and intense convection-radiation interaction with $\varepsilon = 1$. It is perfectly clear that the mean Nusselt number grows with the Rayleigh number for all the cases considered. When the aperture angle is reduced from 45º to 15º (a factor of three), the mean Nusselt number increases remarkably. This behaviour is attributed to an increased conductive heat transfer related to the smaller separation between the hot vertical and cold inclined walls.

The curves in Figure 4 also reveal that for each aperture angle, Nu is nearly invariant with Ra until a critical Rayleigh number Ra_{crit} is attained, which marks the demarcation point between the dominant conduction mode and the onset of the natural convection mode. It is observable in this figure that the critical Rayleigh number Ra_{crit} increases when the aperture angle diminishes.

Finally, those results in Figure 4 manifest that surface radiation is responsible for an elevation in the mean Nusselt number at the hot vertical wall, especially for situations characterized by high Rayleigh numbers. Another effect due to surface radiation is to accelerate the onset of the natural convection mode, i.e., the critical Rayleigh number Ra_{crit} is reduced with respect to those related to a pure natural convection situation.

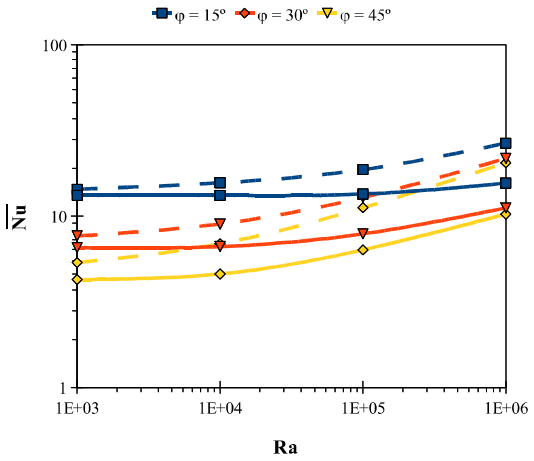

Figure 4 Variation of the mean Nusselt number with the Rayleigh number at the hot vertical wall for three aperture angles 15º, 30º and 45º accounting for the smallest $\varepsilon = 0$ (solid lines) and the largest $\varepsilon = 1$ (dashed lines).

In order to analyze the influence of the working fluid, the results obtained for helium and air (Sieres et al. [5]) have been compared. Shown in Figure 5 is the ratio of the mean Nusselt number at the hot wall when using He and air as working fluids

as a function of the surface emissivities, for the three aperture angles 15º, 30º and 45º. Although these results are for a fixed $Ra = 10^6$, similar trends were found for different Rayleigh values. It can be seen that for pure natural convection, the same value of the mean Nusselt number at the hot wall is obtained when using air or He as the working fluid. When surface radiation is considered, the magnitudes of the mean Nusselt number are higher for air than for He, being this trend accentuated with the emissivity value. However, in terms of the more realistic mean heat transfer coefficient ($\overline{h}$), helium shows always signs of domination and a significant heat transfer augmentation is obtained when replacing air with He as the working fluid. In numbers, for $\varepsilon = 0$ the heat transfer coefficient rendered by He with respect to air delivers an intensification of almost 50% for the three aperture angles under study. When surface radiation is incorporated, this value is reduced and for $\varepsilon = 1$ the heat transfer enhancement is of the order of 24%, 20% and 19% for the 15º, 30º and 45º cavities, respectively.

Owing to page limitations, the interesting plots for the heatlines are not reported but the interested reader may consult the publication by Basak, Aravind and Roy [12].

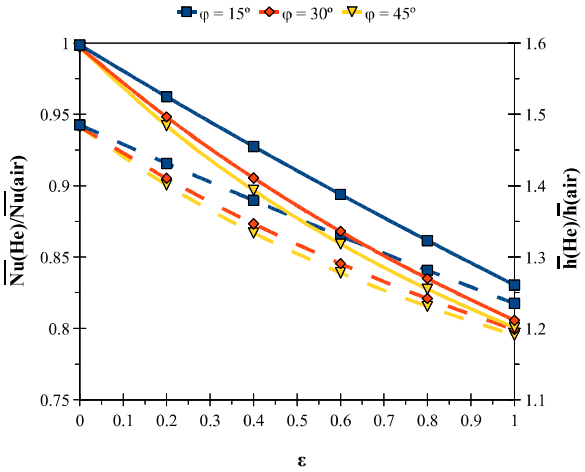

Figure 5 Variation of the mean Nusselt number ratios (solid lines) and the mean heat transfer coefficient ratios (dashed lines) with the surface emissivities for three aperture angles 15º, 30º and 45º at a high $Ra = 10^6$

CONCLUSIONS

In this paper the problem of simultaneous natural convection and surface radiation has been analyzed in a right-angled triangular cavity filled with helium. Several combinations of the height-based Rayleigh number, the aperture angle φ and the surface emissivities ε were studied with the finite volume method. Representative results with/without surface radiation were compared with those obtained with air as the working fluid.

The following major conclusions are drawn from the analysis of the numerical results.

1. For all the combinations analyzed the mean Nusselt number at the hot vertical wall increases with increasing values of the Rayleigh number and with decreasing values of the aperture angle φ.

2. Surface radiation alters the velocity and temperature fields inside the cavity and leads to an elevation of the convective Nusselt number at the hot vertical wall. Designs based on high values of the surface emissivity would result in higher heat transfer rates.

3. A critical Rayleigh number exists that marks the threshold between the conduction mode and the natural convection mode. The critical Rayleigh number decreases for higher aperture angles. Also, it decreases when surface radiation is incorporated.

4. A substantial heat transfer enhancement in terms of the heat transfer coefficient is obtained when replacing air with helium as the working fluid. However, this effect is not seen in terms of the Nusselt number.

REFERENCES

[1] Balaji C. and Venkateshan S.P., Interaction of surface radiation with free convection in a square cavity, *Int. J. Heat Fluid Flow*, Vol. 3, 1993, pp. 260-267.

[2] Akiyama M. and Chong Q.P., Numerical analysis of natural convection with surface radiation in a square enclosure, *Numer. Heat Transfer A*, Vol. 31, 1997, pp. 419-433.

[3] Ramesh N. and Venkateshan S.P., Effect of surface radiation on natural convection in a square enclosure, *J. Thermophys. Heat Transfer*, Vol. 13, 1999, pp. 299-301.

[4] Wang H., Xin S. and Le Quéré P., Etude numérique du couplage de la convection naturelle avec le rayonnement de surfaces en cavité carrée remplie d'air, *Comptes Rendus de Mécanique*, Vol. 334, 2006, pp. 48-57.

[5] Sieres J., Campo A., Ridouane E.H. and Fernández-Seara J., Effect of surface radiation on buoyant convection in vertical triangular cavities with variable aperture angles, *Int. J. Heat Mass Transfer*, Vol. 50, 2007, pp. 5139-5149.

[6] Raithby G.D. and Hollands K.G.T., Natural convection, in: Rohsenow W.M., Harnett J.P. and Cho Y.I. (Eds.), *Handbook of Heat Transfer*, 3rd ed., Mc Graw-Hill, New York, 1998, Chapter 4.

[7] Jaluria Y., Natural convection, in: Bejan A. and Kraus A.D. (Eds.), *Heat Transfer Handbook*, Wiley, New York, 2003, Chapter 7.

[8] Varol Y., Oztop H.F. and Varol A., Free convection in porous media filled right-angle triangular enclosures, *Int. Comm. Heat Mass Transfer*, Vol. 33, 2006, pp. 1190-119.

[9] Versteeg H.K. and Malalasekera W., *An Introduction to Computational Fluid Dynamics*, 2nd ed., Prentice Hall, Harlow, UK, 2007.

[10] Patankar S.V., *Numerical Heat Transfer and Fluid Flow, Hemisphere*, Washington, DC, 1980.

[11] Lemmon E., McLinden M. and Huber M., Reference fluid thermodynamic and transport properties (REFPROP) V 7.0, NIST, 2004.

[12] Basak T., Aravind, G. and Roy, S., Visualization of heat flow due to natural convection within triangular cavities using Bejan's heatline concept, *Int. J. Heat Mass Transfer*, Vol. 52, 2009, pp. 2824-2833.